

**TWO-DIMENSIONAL MODELING OF SINTERING OF A TWO-COMPONENT
METAL POWDER LAYER ON TOP OF MULTIPLE SINTERED LAYERS
WITH A MOVING GAUSSIAN HEAT SOURCE**

Tiebing Chen and Yuwen Zhang
Department of Mechanical Engineering
New Mexico State University
Las Cruces, NM 88003
Reviewed, accepted August 19, 2003

Abstract

Selective Laser Sintering (SLS) of metal powder is modeled as a two-dimensional melting and resolidification of a loose powder layer on top of the sintered metal layers with a moving heat source. The shrinkage induced by melting is accounted for and the problem is modeled using a temperature-transforming model. The results indicate that both the moving heat source intensity and scanning velocity have significant effects on the sintering process. Since the thermal conductivity of the sintered layer is relatively high compared with that of the loose powder, higher heat source intensity and lower scanning velocity are needed to achieve complete melting of the loose powder and bond the current layer to the existing sintered layers. A parametric study is performed and the best combinations of the processing parameters are recommended.

Introduction

Selective Laser Sintering (SLS) is a process that the three-dimensional part is fabricated layer-by-layer from a CAD design [1]. Fabrication of near full density parts from metal powder in the SLS is achieved by melting and resolidification induced by a moving laser beam. A liquid pool is formed when laser beam scans over the top surface of loose powder and then resolidified after the laser beam moves away. Multiple sintered layers, which are fabricated layer by layer due to the reciprocated movement of laser beam, are formed to fabricate three-dimensional part.

Melting and resolidification are the mechanisms to bond powder particles to form a layer of part and they are also the mechanisms to bond different layers together to form a functional part. Fundamentals of melting and solidification have been investigated extensively and detailed reviews are available in the literatures [2, 3]. It should be noted that melting in SLS of metal powder significantly differs from the normal melting process since the significant density change due to the shrinkage accompanies melting. For a single-component powder system, balling phenomenon, which is the formation of small spheres with the approximate diameter of laser beam, occurs since the molten metal is contained by fully loose powder rather than fully dense material. The tensile force on the surface of molten metal is not enough to keep it to a layer-wise geometry. The balling phenomenon can be avoided by using a two-component powder system that contains two types of metal powders possessing significantly different melting points [4, 5]. During the SLS process, only low melting point metal powder goes through melting and resolidification while the high melting point metal powder remains solid in the process. Since the high melting point metal powder alone cannot sustain the powder layer structure, the powder layer collapse upon melting of low melting point metal powder particles. Solidification of low melting point metal bonds the high melting point metal powder particles together to form fully

densified part. The liquid-solid phase change during melting of a two-component packed bed was investigated by Mughal and Plumb numerically [6] and a constant porosity model is developed. Zhang and Faghri [7] analytically solved a one-dimensional melting problem in a semi-infinite powder bed containing a two-component powder mixture subjected to a constant heat flux heating. Chen and Zhang [8] obtained an analytical solution of one-dimensional melting of the two-component metal powder layer with finite thickness.

Since the laser beam is moving over the powder layer and it has a very small diameter compared with the dimension of powder layer, SLS of metal powder is a three-dimensional transient melting and resolidification problem. It is economical to simulate melting and resolidification in a two-dimensional mixed metal powder layer before the real complex three-dimensional model of SLS is developed. A two-dimensional transient model of laser-melting problem with a moving laser beam, of which the interface energy balance was neglect, was developed by Chan et al. [9]. Basu and Srinivasan [10] solved a two-dimensional steady-state laser-melting problem using an alternative direction implicit scheme with a false transient formulation. Melting and resolidification of a subcooled semi-infinite two-component metal powder bed with a moving Gaussian heat source was simulated by Zhang and Faghri [11]. The two-dimensional melting and resolidification problem of a two-component metal powder layer with finite thickness was investigated numerically by Chen and Zhang [12], who demonstrated that the powder layer thickness, moving heat source intensity and scanning velocity have significant effects on the sintering depth. SLS is a process that functional part is fabricated by sintering of powder layer by layer. Except for the first layer, the consecutive layers are always fabricated by sintering of a loose powder layer on top of existing sintered layers. The present paper focuses on the effects of the combination of laser beam intensity and scanning velocity on the sintering process in the loose powder layer when the number of existing sintered layers increases. With prescribed numbers of existing sintered layers, the optimized moving laser beam intensity associated with specified scanning velocity was obtained. A through parametric study will be conducted and an empirical correlation will be proposed.

Physical model and problem statement

A loose powder layer containing two-component metal powders possessing significantly different melting point sits on the top of multiple sintered layers, as shown in Fig. 1. Each existing sintered layer is produced by sintering of two-component metal powder and is considered to be infinite horizontally but finite vertically. A moving Gaussian laser beam interacts with the top surface of the loose powder and then melting is induced. It should be noted that only the low-melting-point-temperature powder melts during the laser sintering process. It is assumed that the sintered layer is fully densified so that the thickness of each sintered layer can be determined by using the thickness and porosity of the loose powder layer. It is very important to identify the best combination of processing parameters that allow complete sintering of the loose powder and secure bonding of the newly sintered layer to existing sintered layer. During the simulation, the sintering depth is permitted to slightly exceed the interface of the loose powder layer and the next existing sintered layer so that each layer can be bonded together tightly.

The following assumptions are made for the physical model:

- (1) Melting and resolidification in SLS is a conduction controlled phase-change problem.

- (2) The thermal properties of the low melting point powder are the same for both liquid and solid phases.
- (3) Two kinds of metal powders are fully mixed and the initial porosity is uniform. The porosity of the sintered layer is zero, which means all of the gas is driven out by shrinkage after the loose powder layer is sintered.
- (4) The bottom of the computational domain is adiabatic.
- (5) The horizontal dimension of the powder layer is sufficiently large compared with the size of the heat source so that the problem is quasi-steady-state.

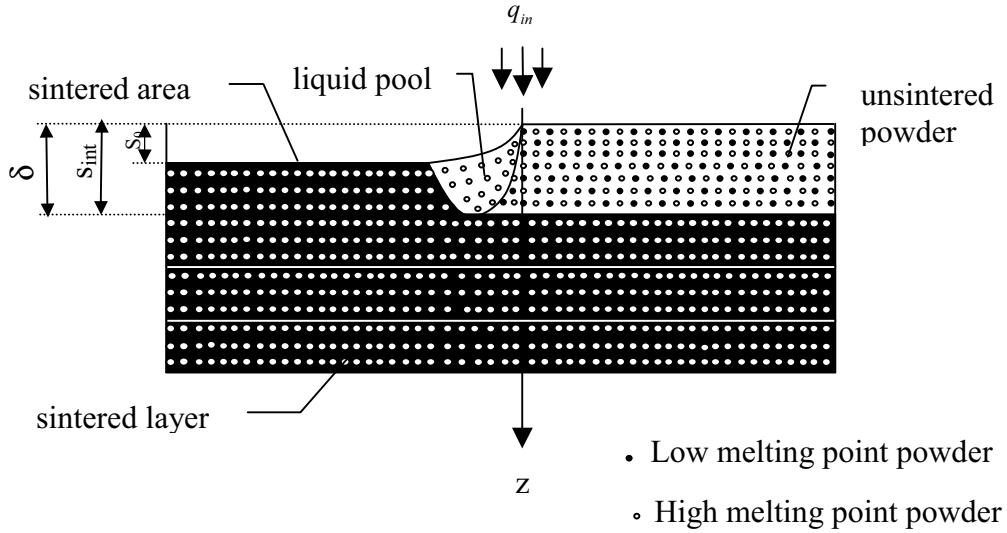


Fig. 1 Physical model

The physical model is formulated using a temperature transforming model, which converts the enthalpy-based energy equation into a nonlinear equation with a single dependent variable - temperature. In this methodology, the solid-liquid phase change is assumed to occur in a very small range of phase-change temperatures from $(T_m^0 - \delta T^0)$ to $(T_m^0 + \delta T^0)$ [13]. The beauty of temperature transforming model is that the converged solution can always be obtained without the limitation on grid size and time step when it deals with the conduction-controlled phase-change problem. It can also successfully model convection controlled solid-liquid phase change problem. A moving coordinate system, of which the origin is fixed at the center of the heat source and moved together with it at the speed, u , is employed. If one observes from the origin, the powder layers travel at a velocity, $-u$, in the opposite moving direction of the laser beam. Therefore, a nonlinear convection term is introduced into the governing equation. Since the horizontal dimension of powder layer is much larger than the size of the heat source, the physical model is a steady-state melting and resolidification problem in a moving coordinate system. The dimensionless governing equation in the moving coordinate system is

$$-U \frac{\partial(CT)}{\partial X} + W \frac{\partial(CT)}{\partial Z} = \frac{\partial}{\partial X} \left(K \frac{\partial T}{\partial X} \right) + \frac{\partial}{\partial Z} \left(K \frac{\partial T}{\partial Z} \right) - \left(-U \frac{\partial S}{\partial X} + W \frac{\partial S}{\partial Z} \right) \quad (1)$$

where the dimensionless variables are defined in the nomenclature. The dimensionless shrinkage velocity, W , heat capacity, C , source term, S , and thermal conductivity, K , in eq. (1) in the

loose powder layer are different from those in existing sintered layers below, which have been fully densitized. In the loose powder layer,

$$W = \begin{cases} -\varepsilon_s U \frac{\partial \eta_{st}}{\partial X} & Z \leq \eta_{st} \leq \Delta \\ 0 & Z > \eta_{st} \leq \Delta \end{cases} \quad (2)$$

$$C = \begin{cases} (1-\varepsilon)(\phi C_L + 1 - \phi) & T < -\Delta T \\ (1-\varepsilon)(\phi C_L + 1 - \phi) + (1-\varepsilon)\phi \frac{C_L}{2Sc\Delta T} & -\Delta T < T < \Delta T \\ (1-\varepsilon)(\phi C_L + 1 - \phi) & T > \Delta T \end{cases} \quad (3)$$

$$S = \begin{cases} 0 & T < -\Delta T \\ \frac{(1-\varepsilon)\phi C_L}{2Sc} & -\Delta T < T < \Delta T \\ \frac{(1-\varepsilon)\phi C_L}{Sc} & T > \Delta T \end{cases} \quad (4)$$

$$K = \begin{cases} K_{eff} & T < -\Delta T \\ K_{eff} + \frac{K_p - K_{eff}}{2\Delta T} (T + \Delta T) & -\Delta T < T < \Delta T \\ K_p & T > \Delta T \end{cases} \quad (5)$$

In the resolidified region at the left side of liquid pool and below the loose powder layer,

$$W = 0 \quad (6)$$

$$C = (1-\varepsilon)(\phi C_L + 1 - \phi) \quad (7)$$

$$S = \frac{(1-\varepsilon)\phi C_L}{Sc} \quad (8)$$

$$K = K_p \quad (9)$$

where K_{eff} is the dimensionless effective thermal conductivity of the loose powder region and K_p is dimensionless thermal conductivity in the sintered region. The mathematical descriptions of K_{eff} and K_p are given in Zhang and Faghri [11]. The corresponding boundary conditions of eq. (1) are as following

$$-K \frac{\partial T}{\partial Z} = N_i \exp(-X^2) - N_R [(T + N_t)^4 - (T_\infty + N_t)^4] - Bi(T - T_\infty) \quad Z = \eta_0(X) \quad (10)$$

$$\frac{\partial T}{\partial Z} = 0, \quad Z = \Delta_s + N \Delta_p, \quad -\infty \leq X \leq \infty, \quad \tau > 0 \quad (11)$$

$$T = -1, \quad |X| \rightarrow \infty, \quad 0 \leq Z \leq \Delta, \quad \tau > 0 \quad (12)$$

The location of liquid surface is related to the sintered depth with the assumption that the sintered layers are fully densitized, i.e.,

$$\eta_0(X) = \varepsilon_s \eta_{st}(X) \quad (13)$$

Numerical Solution

A false transient method is employed to solve eq. (1) numerically since a steady-state problem is difficult to deal with. In this methodology, a false transient term, $\frac{\partial(CT)}{\partial\tau}$, is included in eq. (1) and then the converged steady-state solution is obtained when the temperature distribution and sintering depth do not vary with the false time. Equation (1) with false transient term can be discretised by the finite volume method [14]. A block-off technique recommended by Patankar [14] is employed to deal with the irregular geometry of liquid pool caused by the downward movement of top liquid surface due to shrinkage. Therefore, the computational domain is the regular rectangle and the density and thermal conductivity in the empty space created by the shrinkage are set to zero. The power-law scheme [14] is employed to discretize the convection-diffusion terms. The iteration and underrelaxation are needed in order to obtain the converged solution. A very small dimensionless phase-change temperature range, $\Delta T = 0.001$, is used in the numerical computation.

The dimensionless horizontal length of computational domain is much greater than the magnitude of moving heat source in order to obtain the quasi-steady-state solution. The dimensionless thickness of each existing sintered layer can be determined using the porosity and thickness of loose powder layer as indicated in previous section. The total dimensionless thickness of the whole computational domain in Z direction increases with added numbers of sintered layers. The origin of coordinate system ($X=0, Z=0$) is located at the center of top surface of computational domain in X direction. The non-uniform grids are employed in both of X and Z directions. The numerical solution is carried out for non-uniform grids in X direction of which the fine grids are distributed around the origin symmetrically. The fine grids zone is greater than the width of moving heat source. For the non-uniform grids in Z direction, the fine grids are distributed uniformly in the loose powder layer and the consecutive coarse grids in multiple sintered layers are set up in arithmetic progression with variable grid size according to different numbers of sintered layers. The grid number used in the present paper is 122×32 to 122×47 depending on the number of existing sintered layers. Finer grid sizes were also used but their results did not provide a noticeable difference with the present grid size. It should be noted that finer grids in existing sintered layers is needed in order to obtain the converged solution when too large numbers of sintered layers are concerned, for example, 50 in the present paper.

The optimized combination of heat source intensity and scanning velocity is obtained when the sintering depth penetrates the bottom surface of loose powder layer. In order to trace the sintering depth, a small value of heat source intensity associated with a specific scanning velocity is assigned at first. The dimensionless false time step is assumed to be a value that can not be too large since the convection term is appeared in the governing equation because of the introduced moving coordinate system. The false time step used in the present paper is $\Delta\tau = 0.01$ for $N \leq 10$ and $\Delta\tau = 0.001$ for $N = 50$. The value of heat source intensity is grown with a small increment if the sintering depth is determined not to move further at the previous value of heat source intensity. When the sintering depth approaches the bottom surface of the loose powder layer very closely, the dimensionless false time step and increment of heat source intensity is shifted to a smaller value in order to obtain more accurate solution. The computing procedure is finished when the sintering depth penetrates the bottom surface of loose powder layer.

Results and discussion

The sintering process in a loose powder layer was simulated when the numbers of sintered layers below are 1, 2, 3, 5, 10 and 50 respectively. The effects of dimensionless moving heat source intensity, dimensionless scanning velocity and numbers of sintered layers, which are dominant parameters for a two-dimensional sintering process, were investigated numerically. The effect of subcooling parameter on the sintering process is also investigated.

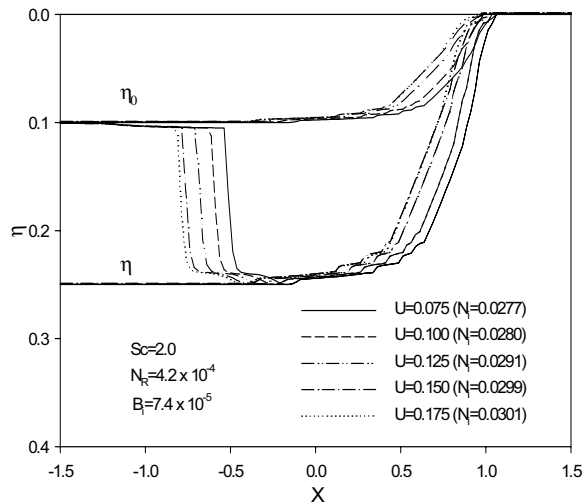


Fig. 2 Combined effects of dimensionless moving heat source intensity and scanning velocity on the sintering process ($N = 1$)

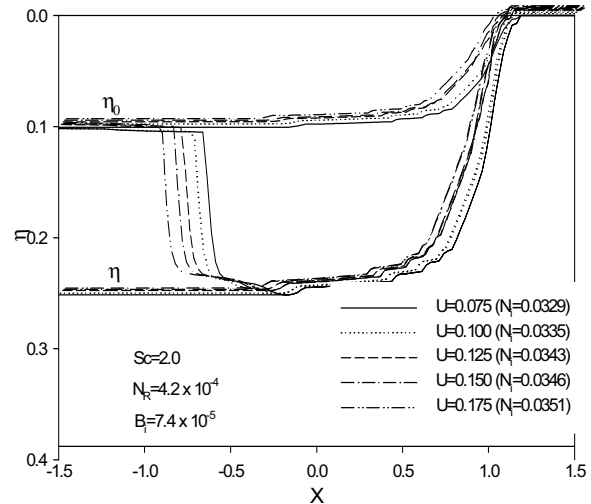


Fig. 3 Combined effects of dimensionless moving heat source intensity and scanning velocity on the sintering process ($N = 2$)

Figure 2 shows the combined effects of dimensionless moving heat source intensity and scanning velocity on the sintering process when there is one sintered layer below. The optimized laser beam intensities is shown in parentheses. The sintering depth penetrates the loose powder layer slightly in order to bond the newly sintered layer to the existing sintered layer. It can be seen that the shape of liquid pools is similar when the scanning velocity increases. The upper part of the liquid pool stretches in the opposite direction of the moving heat source like a tail. The entire liquid pool shifts slightly toward the negative X direction when the scanning velocity increases. The increment of optimized dimensionless heat source intensity is small compared with the increase of scanning velocity from 0.075 to 0.175. It is necessary to let the sintering depth overpass the bottom surface of loose powder layer slightly in order to bond layers together.

The combined effects of dimensionless moving heat source intensity and scanning velocity on the sintering process when there are two sintered layers below are shown in Fig. 3. The shape of the liquid pool at each scanning velocity is similar to those in Fig. 2. When one more sintered layer is added, the heat source intensity at each scanning velocity increases significantly in order to obtain the same sintering depth in the loose powder layer. More heat is conducted away from the loose powder layer since the dimensionless thermal conductivity of sintered part is larger than that of loose powder layer. The numerical simulations are then performed for more sintered layers below and the results are shown in Fig. 4-7. The similar trend of moving heat source intensity at different scanning velocities compared with the corresponding case in Fig. 2 and Fig. 3 can be found. With increasing numbers of sintered layers, the moving heat source intensity at

each scanning velocity is significantly increased. The increment of heat source intensity is similar when the added sintered layer has the same thickness. The liquid pool in the sintering process still keeps the similar shape but its volume is growing because of greater heat source intensity needed. The fluctuation in the front part of liquid pool is growing apparently with increasing numbers of sintered layers below.

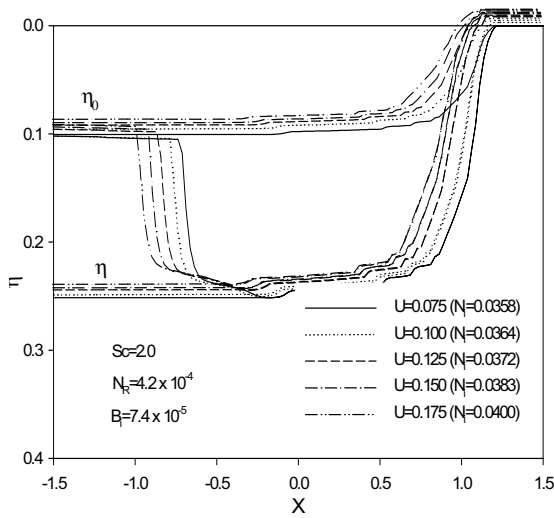


Fig. 4 Combined effects of dimensionless moving heat source intensity and scanning velocity on the sintering process ($N = 3$)

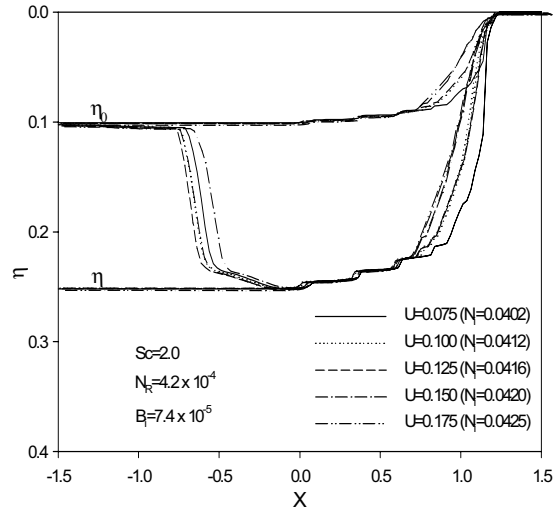


Fig.5 Combined effects of dimensionless moving heat source intensity and scanning velocity on the sintering process ($N = 5$)

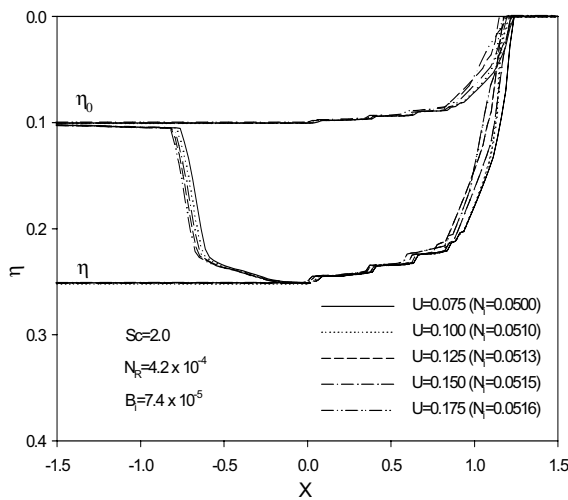


Fig. 6 Combined effects of dimensionless moving heat source intensity and scanning velocity on the sintering process ($N = 10$)

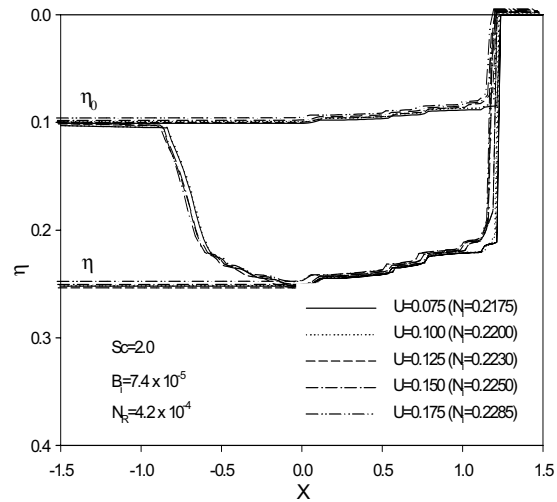


Fig. 7 Combined effects of dimensionless moving heat source intensity and scanning velocity on the sintering process ($N = 50$)

In order to obtain the empirical correlation for the optimized dimensionless moving heat source intensity, a parametric study is performed and the results are shown in Fig. 8. The parameters used to in the simulation are shown in Table 1. The optimized dimensionless moving

heat source intensity is plotted as a function of scanning velocity, U , according to different numbers of sintered layers of which each layer has the same thickness. It can be seen that the optimized dimensionless moving heat source intensity increases with increasing scanning velocity at prescribed numbers of sintered layers and increases significantly when the numbers of sintered layers are added. The optimized dimensionless moving heat source intensity shown in Fig. 8 can be correlated into the following expression,

$$N_i = AU^{-0.0045} + N^{-0.0072} \quad (14)$$

where $A = -0.9627 + 4.3930 \times 10^{-3} N$ and $U > 0$. The error of eq. (14) is within 9.9% .

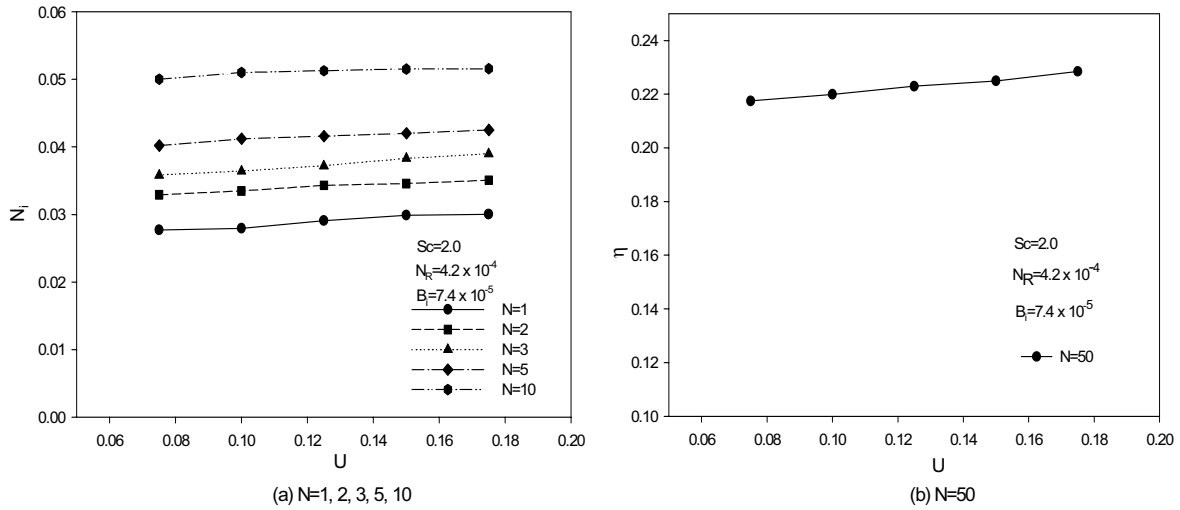


Fig. 8 Optimized dimensionless moving heat source intensity vs. scanning velocity

Table 1 Parameters used in parametric study

ε_s	0.4	N_i	1.5	Sc	2.0	N_i	0.2 ~ 0.4
N_R	4.2×10^{-4}	T_∞	1.0	B_i	7.4×10^{-5}	U	0.075 ~ 0.175
Δ_s	0.25	ϕ	0.4	K_{LH}	2.9	C_{LH}	0.7
N	1, 2, 3, 5, 10, 50						

In order to investigate the effect of preheating on the sintering process, effect of subcooling parameter on the sintering process is studied and the results are shown in Fig 9, in which the number of existing sintered layers below is fixed at one. The optimized dimensionless moving heat source intensity to achieve the same sintering depth decreases when the lower subcooling parameter is employed. The shape of liquid pool keeps similar when the lower subcooling parameter is used. At lower subcooling parameter, the initial temperature is closing to the melting point of the low-melting-point metal powder. The lower subcooling parameter is

beneficent to the sintering process since not only the moving heat source intensity needed is reduced but also the pre-heating time is shortened.

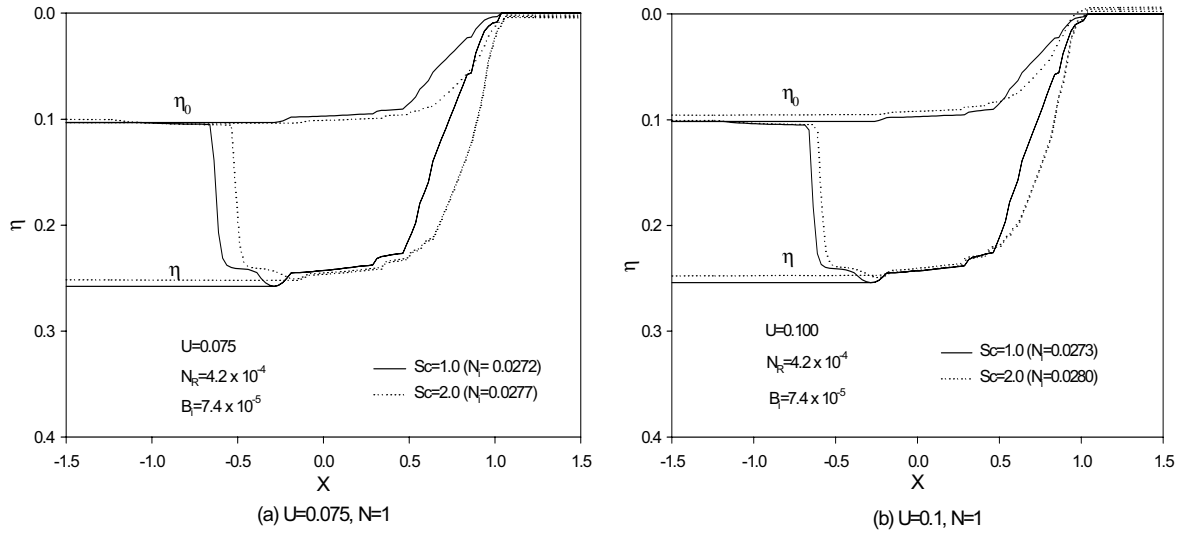


Fig. 9 Effect of subcooling number on the sintering process

Conclusions

A parametric study of a two-dimensional SLS process in a loose powder layer on top of multiple sintered metal powder layers is presented. The results showed that the optimized dimensionless moving heat source intensity increases with increasing scanning velocity in order to achieve the desired sintering depth to bond the newly sintered layer to the existing sintered layer. With increasing numbers of existing sintered layers below, the optimized dimensionless moving heat source intensity at a specific scanning velocity increases significantly. An empirical correlation on the dimensionless moving heat source intensity is obtained. The optimized dimensionless moving heat source intensity decreases when the lower subcooling parameter is used.

Acknowledgement

Support for this work by the Office of Naval Research under grant number N00014-02-1-0356 is greatly acknowledged.

Nomenclature

- b moving heat source half width (m)
- Bi Biot number, hb/k_H
- C dimensionless heat capacity, C^0/C_H^0
- C^0 heat capacity, ρc_p
- c_p specific heat, ($W/kg K$)
- h convective heat transfer coefficient, ($W/m^2 K$)
- h_m latent heat of melting or solidification, J/kg

I_0	heat source intensity at the center of the heat source, (W / m^2)
k	thermal conductivity, $(W / m K)$
K	dimensionless thermal conductivity, k / k_H
N	numbers of sintered layers under the loose powder layer
N_i	dimensionless moving heat source intensity, $\alpha_a I_0 b / [k_H (T_m^0 - T_i^0)]$
N_R	Radiation number, $\varepsilon \sigma (T_m^0 - T_i^0)^3 b / k_H$
N_t	temperature ratio for radiation, $T_m^0 / (T_m^0 - T_i^0)$
s	solid-liquid interface location (m)
s_0	location of surface (m)
s_{st}	sintered depth (m)
Sc	subcooling parameter, $C_H^0 (T_m^0 - T_i^0) / (\rho_L h_{sl})$
T	dimensionless temperature, $(T^0 - T_m^0) / (T_m^0 - T_i^0)$
t	false time (s)
T^0	temperature (K)
u	heat source moving velocity (m / s)
U	dimensionless heat source moving velocity, ub / α_H
V	volume (m^3)
w	velocity of liquid phase (m / s)
W	dimensionless velocity of the liquid phase, wb / α_H
x	moving horizontal coordinate
X	dimensionless moving horizontal coordinate, x / b
z	vertical coordinate (m)
Z	dimensionless vertical coordinate, z / b

Greek symbol

α	thermal diffusivity $(m^2 s^{-1})$
δ	powder layer thickness, m
Δ	dimensionless powder layer thickness, δ / b
ΔT^0	one-half of phase-change temperature range (K)
ΔT	one-half of dimensionless phase change temperature range
ε	volume fraction of gas (porosity for unsintered powder), $V_g / (V_g + V_L + V_H)$
ε_e	emissivity of surface
η	dimensionless solid-liquid interface location, s / b
η_0	dimensionless location of the surface, s_0 / b
η_{st}	dimensionless sintered depth, s_{st} / b
ρ	density (kg / m^3)
σ	Stefan-Boltzman constant, $5.67 \times 10^{-8} W / (m^2 K^4)$
τ	false dimensionless time, $\alpha_H t / b^2$
ϕ	volume percentage of low melting point powder, $V_L / (V_L + V_H)$

Subscripts

<i>eff</i>	effective
<i>H</i>	high melting point powder
<i>L</i>	low melting point powder
<i>m</i>	melting point
<i>p</i>	sintered parts
<i>s</i>	solid

References

- [1] Conley, J., and Marcus, H., 1997, "Rapid Prototyping and Solid Freeform Fabrication," *Journal of Manufacturing Science and Engineering*, Vol. 119, pp. 811-816.
- [2] Viskanta, R., 1983, Phase Change Heat Transfer, in: G.A. Lane (Ed.), *Solar Heat Storage: Latent Heat Materials*, CRC Press, Boca Raton, FL.
- [3] Yao, L., and Prusa, J., 1989 "Melting and freezing," *Advances in Heat Transfer*, Vol. 25, pp. 1-96.
- [4] Manzur, T., DeMaria, T., Chen, W., and Roychoudhuri, C., 1996, "Potential Role of High Powder Laser Diode in Manufacturing," presented at SPIE Photonics West Conference, San Jose, CA
- [5] Bunnell, D., 1995, *Fundamentals of Selective Laser Sintering of Metals*, Ph.D. Thesis, University of Texas at Austin.
- [6] Mughal, M., and Plumb, O. A., 1993, "Thermal Densification of Metal-Ceramic Composites," *Scripta Metallurgica et Materialia*, Vol. 29, pp. 383-388.
- [7] Zhang, Y., and Faghri, A., 1999, "Melting of a Subcooled Mixed powder Bed with Constant Heat Flux Heating," *International Journal of Heat and Mass Transfer*, Vol. 42, pp. 775-788.
- [8] Chen, T., and Zhang, Y., 2003, "Analysis of Melting in a Mixed Powder Bed with Finite Thickness Subjected to Constant Heat Flux Heating," *Proceeding of ASME Summer Heat Transfer Conference*, Las Vegas, NV.
- [9] Chan, C., Mazumder, J., and Chen, M., 1984, "A Two Dimensional Transient Model for Convection in Laser Melted Pool," *Metall. Trans.*, Vol. 15A, pp. 2175-2184.
- [10] Basu, B., and Srinivasan, J., 1988, "Numerical Study of Steady-State Laser Melting Problem," *Int. J Heat Mass Transfer*, Vol. 31, No.11, pp. 2331-2338.
- [11] Zhang, Y., and Faghri, A., 1998, "Melting and Resolidification of a Subcooled Mixed Powder Bed with Moving Gaussian Heat Source," *ASME Journal of Heat Transfer* Vol. 120, pp. 883-891.
- [12] Chen, T. and Zhang, Y., 2003, "Melting and Resolidification of a Two-Component Metal powder Layer Heated by a Moving Gaussian Heat Source," IMECE2003, Washington, DC.
- [13] Cao, Y. and Faghri, A., 1990, "A Numerical Analysis of Phase Change Problems Including Natural Convection," *Journal of Heat Transfer*, Vol. 112, pp. 812-816.
- [14] Patankar, S. V., 1980, *Numerical Heat Transfer and Fluid Flow*, McGraw-Hill, New York.